The Radioprotective 105/MD-1 Complex Contributes to Diet-Induced Obesity and Adipose Tissue Inflammation

Yasuharu Watanabe,[1] Tomoya Nakamura,[1] Sho Ishikawa,[1] Shiho Fujisaka,[2] Isao Usui,[2] Koichi Tsuneyama,[3] Yoshinori Ichihara,[4] Tsutomu Wada,[4] Yoichiro Hirata,[5] Takayoshi Suganami,[6] Hirofumi Izaki,[7] Shizuo Akira,[8] Kensuke Miyake,[9] Hiro-omi Kanayama,[7] Michio Shimabukuro,[10] Masataka Sata,[5] Toshiyasu Sasaoka,[4] Yoshihiro Ogawa,[6] Kazuyuki Tobe,[2] Kiyoshi Takatsu,[1,11] and Yoshinori Nagai[1]

Recent accumulating evidence suggests that innate immunity is associated with obesity-induced chronic inflammation and metabolic disorders. Here, we show that a Toll-like receptor (TLR) protein, radioprotective 105 (RP105)/myeloid differentiation protein (MD)-1 complex, contributes to high-fat diet (HFD)-induced obesity, adipose tissue inflammation, and insulin resistance. An HFD dramatically increased RP105 mRNA and protein expression in stromal vascular fraction of epididymal white adipose tissue (eWAT) in wild-type (WT) mice. RP105 mRNA expression also was significantly increased in the visceral adipose tissue of obese human subjects relative to nonobese subjects. The RP105/MD-1 complex was expressed by most adipose tissue macrophages (ATMs). An HFD increased RP105/MD-1 expression on the M1 subset of ATMs that accumulate in eWAT. Macrophages also acquired this characteristic in coculture with 3T3-L1 adipocytes. RP105 knockout (KO) and MD-1 KO mice had less HFD-induced adipose tissue inflammation, hepatic steatosis, and insulin resistance compared with wild-type (WT) and TLR4 KO mice. Finally, the saturated fatty acids, palmitic and stearic acids, are endogenous ligands for TLR4, but they did not activate RP105/MD-1. Thus, the RP105/MD-1 complex is a major mediator of adipose tissue inflammation independent of TLR4 signaling and may represent a novel therapeutic target for obesity-associated metabolic disorders. ***Diabetes*** **61:1199–1209, 2012**

From the [1]Department of Immunobiology and Pharmacological Genetics, Graduate School of Medicine and Pharmaceutical Science for Research, University of Toyama, Toyama, Japan; the [2]Department of First Internal Medicine, Graduate School of Medicine and Pharmaceutical Science for Research, University of Toyama, Toyama, Japan; the [3]Department of Diagnostic Pathology, Graduate School of Medicine and Pharmaceutical Science for Research, University of Toyama, Toyama, Japan; the [4]Department of Clinical Pharmacology, Graduate School of Medicine and Pharmaceutical Science for Research, University of Toyama, Toyama, Japan; the [5]Department of Cardiovascular Medicine, Institute of Health Biosciences, The University of Tokushima Graduate School, Tokushima, Japan; the [6]Department of Molecular Medicine and Metabolism, Medical Research Institute, Tokyo Medical and Dental University, Tokyo, Japan; the [7]Department of Urology, Institute of Health Biosciences, The University of Tokushima Graduate School, Tokushima, Japan; the [8]Laboratory of Host Defense, WPI Immunology Frontier Research Center, Osaka University, Osaka, Japan; the [9]Division of Infectious Genetics, Department of Microbiology and Immunology, The Institute of Medical Science, The University of Tokyo, Tokyo, Japan; the [10]Department of Cardio-Diabetes Medicine, Institute of Health Biosciences, The University of Tokushima Graduate School, Tokushima, Japan; and the [11]Toyama Prefectural Institute for Pharmaceutical Research, Toyama, Japan.

Corresponding authors: Yoshinori Nagai, ynagai@med.u-toyama.ac.jp, and Kiyoshi Takatsu, takatsuk@med.u-toyama.ac.jp.

Received 24 August 2011 and accepted 3 February 2012.

DOI: 10.2337/db11-1182

This article contains Supplementary Data online at http://diabetes.diabetesjournals.org/lookup/suppl/doi:10.2337/db11-1182/-/DC1.

Y.W., T.N., and Y.N. contributed equally to this work.

Y.N. and K.Ta. are both senior authors.

T.N. is currently affiliated with the R&D Center, Ikeda Mohando, Toyama, Japan.

Y.H. is currently affiliated with the Department of Pediatrics, Graduate School of Medicine, The University of Tokyo, Tokyo, Japan.

Obesity is associated with chronic low-grade inflammation characterized by increased proinflammatory cytokines and infiltration of macrophages within adipose tissue (1), leading to insulin resistance (2). Although several inflammatory mediators and cell types promote these processes, precise roles of the immune system are not fully understood. Most of the infiltrated adipose tissue macrophages (ATMs) in obese adipose tissue are CD11c-positive inflammatory M1 macrophages responsible for the development of adipose tissue inflammation, which is countered by CD206-positive anti-inflammatory M2 macrophages (3,4).

Pattern recognition receptors (PRRs) such as Toll-like receptors (TLRs) quickly recognize pathogenic agents called pathogen-associated molecular patterns (5). The TLR4/myeloid differentiation protein (MD)-2 complex is indispensable for lipopolysaccharide (LPS) recognition (6,7). TLR4 requires two important adaptor molecules, myeloid differentiation factor 88 (MyD88) and TIR-domain-containing adaptor-inducing interferon-β (TRIF), to transmit its downstream signaling (5). A TLR4 homolog, radioprotective 105 (RP105), forms a complex with MD-1 (8,9). RP105 or MD-1 knockout (KO) mice show reduced proliferative responses to LPS in B cells and are impaired in hapten-specific antibody production against LPS (10–12), suggesting that the RP105/MD-1 complex cooperates with the TLR4/MD-2 complex in LPS responses. RP105/MD-1 also is expressed on macrophages (12). However, roles for RP105/MD-1 in chronic inflammation–associated metabolic disorders have not been suspected.

PRRs also can sense endogenous ligands called danger-associated molecular patterns. These include intracellular molecules such as fatty acids (FAs), heat shock proteins, and host nucleic acids, as well as extracellular components, such as hyaluronan and proteoglycans (13). These molecules can ligate PRRs, leading to activation of proinflammatory pathways and cytokine secretion. This often is referred to as "sterile" inflammation (14).

Adipose tissue–derived saturated free FAs may stimulate TLR4 and promote adipose tissue inflammation and insulin resistance (15–17). The Nlrp3 (nucleotide-binding domain, leucine-rich repeats containing family, pyrin domain-containing-3) inflammasome senses obesity-associated FAs and contributes to obesity-induced inflammation and insulin resistance (18,19). Double-stranded RNA-dependent protein kinase can sense FAs from nutrients as well as endoplasmic reticulum stress and plays critical roles in regulating insulin action and metabolism (20). Of interest, the G-protein–coupled receptor 120 recognizes unsaturated

omega-3 FAs (docosahexaenoic acid and eicosapentaenoic acid) and mediates insulin sensitizing by suppressing macrophage-induced inflammation (21). However, it remains unclear whether RP105/MD-1 has a role in sensing obesity-related natural ligand or whether the complex participates in immune responses leading to diet-induced chronic inflammation and insulin resistance.

We now report that RP105 or MD-1 KO mice were protected from high-fat diet (HFD)-induced obesity, hepatic steatosis, insulin resistance, and adipose tissue inflammation. RP105/MD-1 was expressed on macrophages in the stromal vascular fraction (SVF) of epididymal white adipose tissue (eWAT). RP105 mRNA expression was significantly increased in the visceral adipose tissue (VAT) of obese subjects. An HFD and coculture with adipocytes dramatically increased the expression of RP105 by macrophages. Endogenous TLR4 ligands, palmitic and stearic acids, did not stimulate RP105/MD-1. Therefore, the RP105/MD-1 receptor complex contributes in unique ways to diet-induced obesity and related inflammatory responses.

RESEARCH DESIGN AND METHODS

Mice. C57BL/6 mice were purchased from Japan SLC (Hamamatsu, Japan) and were used at 10 weeks of age. Mice were fed an HFD containing 60% fat (Research Diet, New Brunswick, NJ) or a standard diet containing 10% fat starting at 10 weeks of age for 12 weeks. Male mice were maintained in microisolator cages under specific pathogen-free conditions with a 12-h light/12-h dark cycle in the animal facility of University of Toyama and given free access to food and water. All experiments were performed according to the guidelines for the care and treatment of experimental animals at the University of Toyama.

Reagents. LPS from *Escherichia coli* O55:B5, palmitic, stearic, and lauric acids were purchased from Sigma-Aldrich (St. Louis, MO).

Human study. A total of 18 Japanese male patients with urological diseases who received surgery in Tokushima University Hospital were recruited in this study (Supplementary Table 1). Adipose tissue around the kidney or prostate was obtained as VAT samples. Subcutaneous adipose tissue (SAT) samples were obtained from the abdominal walls during urological surgery. This study protocol was approved by the ethics committee on human research of the University of Tokushima Graduate School and University of Toyama.

Metabolic measurements. Serum total cholesterol and alanine transaminase (ALT) were measured by Reflotron-plus (Roche Diagnostics, Mannheim, Germany). The glucose tolerance test (GTT) was performed by intraperitoneally injecting 1 g glucose/kg. For the insulin tolerance test (ITT), the mice were injected with 0.75 units of human insulin/kg i.p. (Eli Lilly, Indianapolis, IN). Blood glucose was measured by NIPRO FreeStyle FLASH (NIPRO, Osaka, Japan), and serum insulin was measured by an enzyme-linked immunosorbent assay kit (Shibayagi, Shibukawa, Japan).

Measurement of V_{O_2}, V_{CO_2}, and respiratory quotient. Mice were placed in standard metabolic cages (model MK5000RQ; Muromachikikai, Tokyo, Japan) with an airflow of 0.5 L/min. Oxygen consumption (V_{O_2}) and carbon dioxide production (V_{CO_2}) were measured during 3 consecutive days (three dark cycles and two light cycles). Respiratory quotient (R_Q) was calculated as a ratio of V_{CO_2} to V_{O_2}.

Isolation of adipocytes and SVF from eWAT. Mice were fasted for 12 h before dissection. Isolation of adipocytes and SVF was performed as described previously (4).

Flow cytometry analysis. The cells (1×10^5) were incubated with anti-mouse FcγR (2.4G2) to block binding of the labeled antibodies to FcγR. After 15 min, the cells were stained with predetermined optimal concentrations of the respective antibodies. 7-Amino-actinomycin D (BD Bioscience, San Diego, CA) was used to exclude dead cells. Flow cytometry analyses were conducted on a FACSCanto (Becton Dickinson, Mountain View, CA), and the data were analyzed with Flowjo software (Treestar, San Carlos, CA). The information for antibodies is listed in Supplementary Table 2.

Cell culture. RAW264.7 cells (RIKEN BioResource Center, Tsukuba, Japan) and 3T3-L1 cells (American Type Culture Collection, Manassas, VA) were maintained with DMEM containing 10% fetal calf serum and antibiotics and incubated at 37°C in a humidified 5% CO_2. 3T3-L1 cells were differentiated based on a standard protocol (22). Bone marrow–derived macrophages (BMMs) were differentiated into M1 and M2 macrophages as described previously (23).

Coculture of adipocytes and macrophages. Coculture of 3T3-L1 cells and macrophages was performed as described previously (17). RAW264.7 cells were cocultured with the 3T3-L1 cells in the absence or presence of pioglitazone (Funakoshi, Tokyo, Japan) for 24 h.

Real-time quantitative PCR. Total RNA was isolated with an RNeasy mini kit (Qiagen, Hilden, Germany) or TRIzol Reagent (Invitrogen, Carlsbad, CA). RNA was reverse transcribed with a TaqMan Reverse Transcription Reagents (Applied Biosystems, Carlsbad, CA). Real-time quantitative PCR (RT-qPCR) was performed with a TaqMan Gene Expression Master Mix (Applied Biosystems) and analyzed with an Mx3000P (Agilent Technologies, Santa Clara, CA). Relative transcript abundance was normalized for that of Hprt mRNA. The information for primers is listed in Supplementary Table 3.

Immunoprecipitation and Western blot analysis. The immunoprecipitation for RP105 was performed by using anti-RP105 (RP/14) (24). To detect RP105 by Western blotting, the anti-RP105 (0.5 μg/mL) (ProSci, Poway, CA) and horseradish peroxidase–conjugated anti-rabbit IgG (Cell Signaling, Beverly, MA) were used. Anti-actin was purchased from Sigma-Aldrich. The reactive bands were visualized by ECL Plus (GE Healthcare, Little Chalfont, Bucks, U.K.).

Immunohistochemistry analysis. Portions of the liver and eWAT were excised and immediately fixed with 4% formaldehyde at room temperature. Paraffin-embedded tissue sections were cut into 4-mm slices and placed on slides. CD11c staining was performed as described previously (4). The sections were incubated with anti–Mac-2 (macrophage surface glycoproteins binding to galectin-3), anti–MD-1 (MD113), or anti-RP105 (ProSci) for 1 h and then with ready-to-use polymered secondary antibodies for rat or rabbit monoclonal antibodies with peroxydase (Envision-PO; Dako, Glostrup, Denmark) for 1 h. Bound antibodies were detected with 3,3′-diaminobenzidine. Sections were counterstained with hematoxylin.

Statistical analysis. Statistical significance was evaluated by one-way ANOVA followed by a post hoc Tukey test. $P < 0.05$ was considered statistically significant.

RESULTS

RP105 expression dramatically increases in the adipose tissue from HFD-fed mice and obese subjects. Our initial studies evaluated the expression of genes encoding RP105/MD-1, TLRs, MD-2, and components involved in TLR signaling in the eWAT from WT mice fed with a normal diet (ND) or an HFD (Fig. 1*A*). HFD treatment markedly increased the expression of RP105 mRNA by 13-fold. The expression of MD-1, TLR1, TLR7, TLR8, and TLR9 mRNA also was increased by HFD, whereas the expression of TLR4 and MD-2 mRNA was not affected. The MyD88 and TRIF are critical adaptor molecules for TLR4 signaling (5) but are not involved in RP105 signaling (data not shown). MyD88 and TRIF mRNA, as well as TLR4 mRNA, were not increased by an HFD in eWAT (Fig. 1*A*). RP105 and MD-1 mRNAs also were significantly increased in other WAT depots, such as subcutaneous and retroperitoneal WAT, by an HFD (Supplementary Fig. 1). Levels of TLR4 mRNA in retroperitoneal adipose tissue were slightly increased by an HFD. HFD also increased RP105 mRNA in the liver, brown adipose tissue, and skeletal muscle by 1.6-, 3-, and 1.7-fold, respectively (Supplementary Fig. 2). In addition, the expression of RP105 and MD-1 mRNA in the spleen and bone marrow was not significantly affected by an HFD. Expression of TLR4, MD-2, MyD88, and TRIF in these tissues was not significantly affected by an HFD.

To test the clinical relevance of data generated from mouse models, we examined RP105 and MD-1 mRNA expression in human adipose tissue. Linear regression analyses showed a positive correlation between RP105 mRNA levels and BMI in the VAT but not the SAT (Fig. 1*B*). RP105 mRNA expression was increased in the VAT but not the SAT of obese subjects relative to nonobese subjects (Fig. 1*C*). In contrast, MD-1 mRNA expression was significantly increased in the SAT but not the VAT of obese subjects (Supplementary Fig. 3).

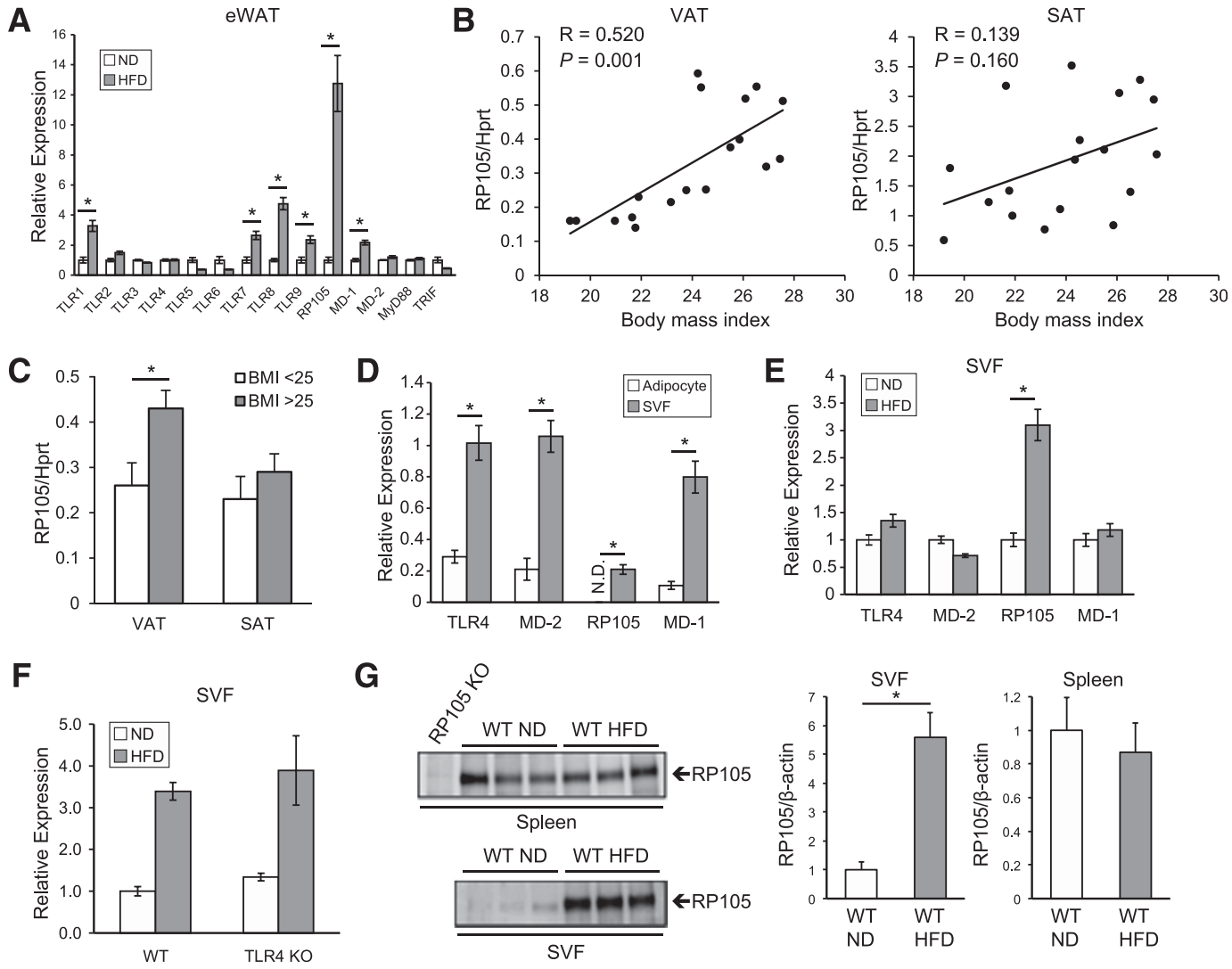

FIG. 1. RP105 and MD-1 expression in mouse and human adipose tissues. ***A*****: RT-qPCR of TLRs, RP105/MD-1, MD-2, MyD88, and TRIF mRNA in the eWAT from WT fed with an ND or HFD for 12 weeks (n = 8 per group). Data are presented relative to the expression in ND-fed mice, set as 1. Data are shown as means ± SE. *P < 0.05 vs. ND.** ***B*****: Linear regression analysis of the correlation between adipose RP105 mRNA expression and BMI.** ***C*****: RP105 mRNA expression of the human adipose tissue of nonobese (BMI <25 kg/m^2; n = 11) and obese (BMI >25 kg/m^2; n = 7) subjects. Data are shown as means ± SE. *P < 0.05.** ***D*****: RT-qPCR of TLR4, MD-2, RP105, and MD-1 mRNA in adipocytes and SVF from WT mice on an ND (n = 8 per group). Data are shown as means ± SE. *P < 0.05 vs. adipocyte. N.D., not detected.** ***E*****: RT-qPCR of TLR4, MD-2, RP105, and MD-1 mRNA in SVF from WT mice on an ND or HFD for 12 weeks (n = 8 per group). Data are presented relative to the expression in the ND, set as 1. Data are shown as means ± SE. *P < 0.05 vs. ND.** ***F*****: RT-qPCR of RP105 mRNA in SVF from WT or TLR4 KO mice fed with an ND or HFD for 12 weeks (n = 7 per group). Data are presented relative to the expression in WT mice fed with an ND, set as 1. Data are shown as means ± SE.** ***G*****: Immunoprecipitation analysis of RP105 in lysates of spleen (2 × 10^7 cells/lane) or SVF (2 × 10^6 cells/lane) from WT mice on an ND or HFD for 12 weeks. Data are presented as means ± SE normalized to β-actin expression (bar graphs). *P < 0.05 vs. WT ND.**

To determine the nature of RP105-bearing cells in eWAT, we isolated adipocytes and the SVF from the eWAT of WT mice (Fig. 1*D*). In adipocytes, MD-1, TLR4, and MD-2 mRNA were expressed, whereas RP105 mRNA was not detected. The SVF expressed all the tested genes, but the level of RP105 mRNA was lower than those of others. In SVF, only RP105 was increased by an HFD (Fig. 1*E*). In addition, this change was independent of TLR4 signaling, as it was present in KO mice lacking TLR4 (Fig. 1*F*). Likewise, RP105 protein levels were increased in obese mice compared with lean mice (Fig. 1*G*). This change was not detected in the spleen. These results indicate that the expression of RP105 is associated with diet-induced obesity.

The RP105/MD-1 complex is expressed in ATMs. We then traced the expression of RP105 and MD-1 in SVF cells. Approximately 40% of the SVF cells from ND-fed mice were composed of CD45$^+$ cells, and the percentage increased to ~55% by HFD (Fig. 2*A*). In contrast, an HFD decreased the percentage of CD45$^-$ cells. RP105 and MD-1 were seen on CD45$^+$ but not CD45$^-$ cells in ND-fed mice (Fig. 2*B*). Those leukocytes were heterogeneous with respect to RP105 and MD-1 densities, and the percentages of RP105- and MD-1–bearing cells increased by HFD. The TLR4/MD-2 complex was not displayed by either CD45$^+$ or CD45$^-$ cells. The staining intensity of RP105 correlated with that of MD-1 (Fig. 2*C*). There was good correlation between transcript expression and flow cytometry results (Supplementary Fig. 4). Of interest, CD45$^-$ cells had TLR4 and MD-2 mRNA, and an HFD increased MD-2 mRNA in CD45$^-$ cells by approximately threefold.

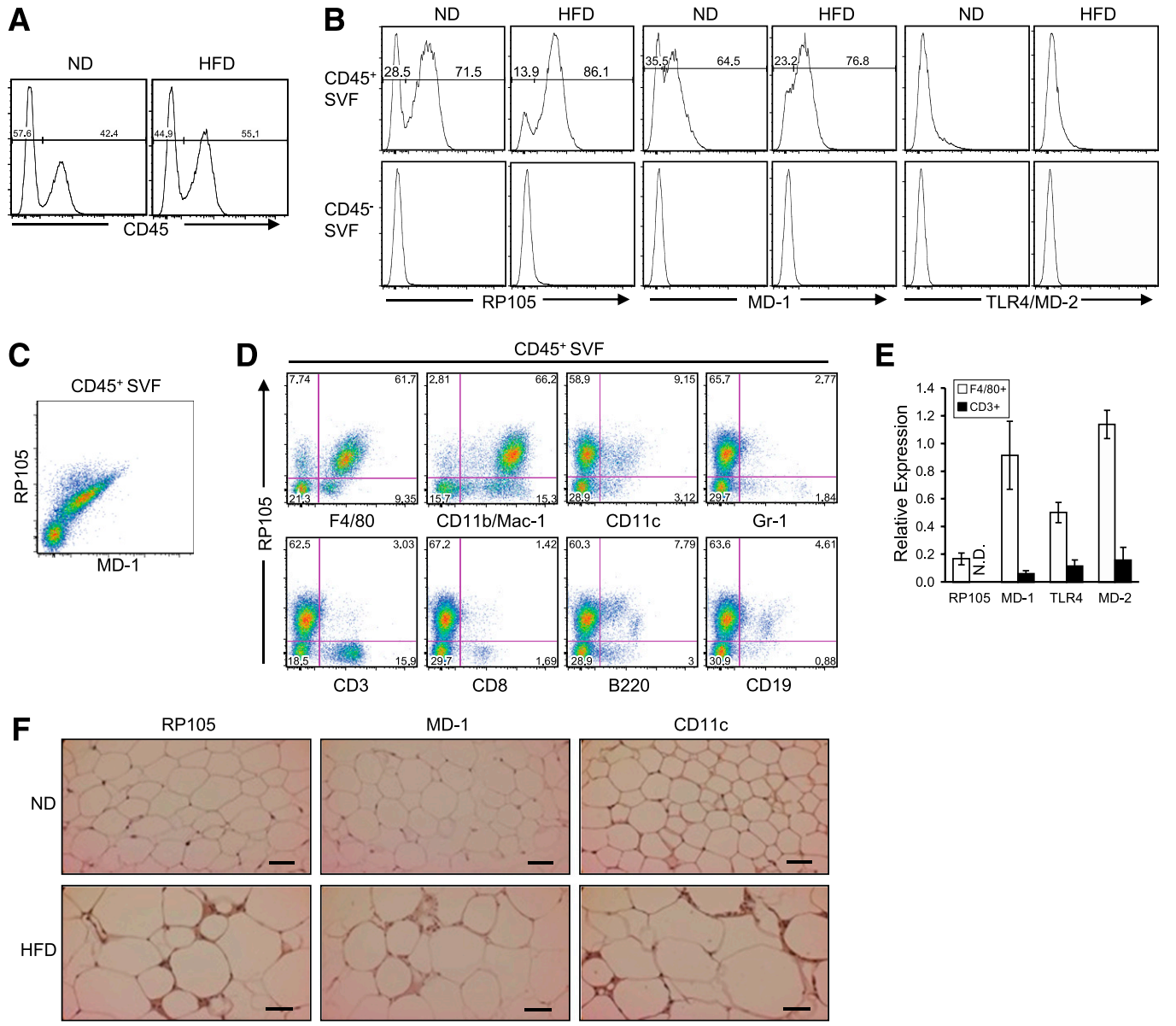

FIG. 2. ATMs are major RP105/MD-1-expressing cells in SVF. *A*: Flow cytometry analysis of CD45 expression on SVF cells from WT mice on an ND or HFD for 12 weeks. *B*: Flow cytometry analysis of RP105, MD-1, and TLR4/MD-2 expression on CD45$^+$ or CD45$^-$ SVF cells from WT mice on an ND or HFD for 12 weeks. *C*: Flow cytometry analysis of RP105 and MD-1 expression on CD45$^+$ SVF cells from WT mice on an ND. *D*: Flow cytometry analysis of CD45$^+$ SVF cells from WT mice on an ND. *E*: RT-qPCR of RP105, MD-1, TLR4, and MD-2 mRNA in F4/80$^+$ or CD3$^+$ SVF cells from WT mice on an ND. Data are shown as means ± SE. N.D., not detected. *F*: Representative histological images of eWAT from WT mice on an ND or HFD for 12 weeks stained with RP105, MD-1, and CD11c. Scale bars, 50 μm (ND) and 100 μm (HFD). All data are representative of at least two independent experiments. (A high-quality digital representation of this figure is available in the online issue.)

Additional flow cytometry analyses revealed that a majority of the RP105-expressing CD45$^+$ cells were F4/80$^+$ and CD11b/Mac-1$^+$ (Fig. 2*D*). Some RP105-expressing cells were CD11c, B220, and CD19 positive. CD8$^+$ T cells have been reported to promote the recruitment and activation of macrophages in adipose tissue (25). However, CD3$^+$ and CD8$^+$ cells did not have detectable RP105 (Fig. 2*D*). CD3$^+$ cells had no RP105 and low MD-1 mRNA (Fig. 2*E*). In addition, RP105 and MD-1 were made by CD11b/Mac-1$^+$ and CD19$^+$ cells but not CD3$^+$ cells in spleen cells of WT animals (Supplementary Fig. 5*A* and *B*). RP105 and MD-1 were predominantly expressed in ATM clusters in eWAT from HFD-fed mice (Fig. 2*F*). These RP105-/MD-1–positive cells also stained positive for CD11c. It is clear from these findings that majority of RP105-/MD-1–expressing SVF cells is ATMs.

Expression of RP105 and MD-1 on M1 macrophages reflects differentiation and is regulated by HFD and adipocytes. Additional information about RP105/MD-1 expression was obtained by examination of M1 and M2 macrophage subsets (Fig. 3*A*). Differentiated M1 macrophages were strongly positive for RP105 and MD-1 as well as tumor necrosis factor (TNF)-α and inducible nitric oxide synthase, representative M1 markers. MD-2 mRNA also was significantly increased by M1 differentiation. In contrast to the expression of arginase 1 and Mgl2 mRNA, the levels of RP105 and MD-1 mRNA in M2 were similar to those in undifferentiated BMMs. TLR4 and MD-2 mRNA were not significantly influenced by M2 differentiation. The RP105/MD-1 complex was detected on M1 and M2 ATMs from ND-fed mice (Fig. 3*B*). Of interest, RP105/MD-1 on

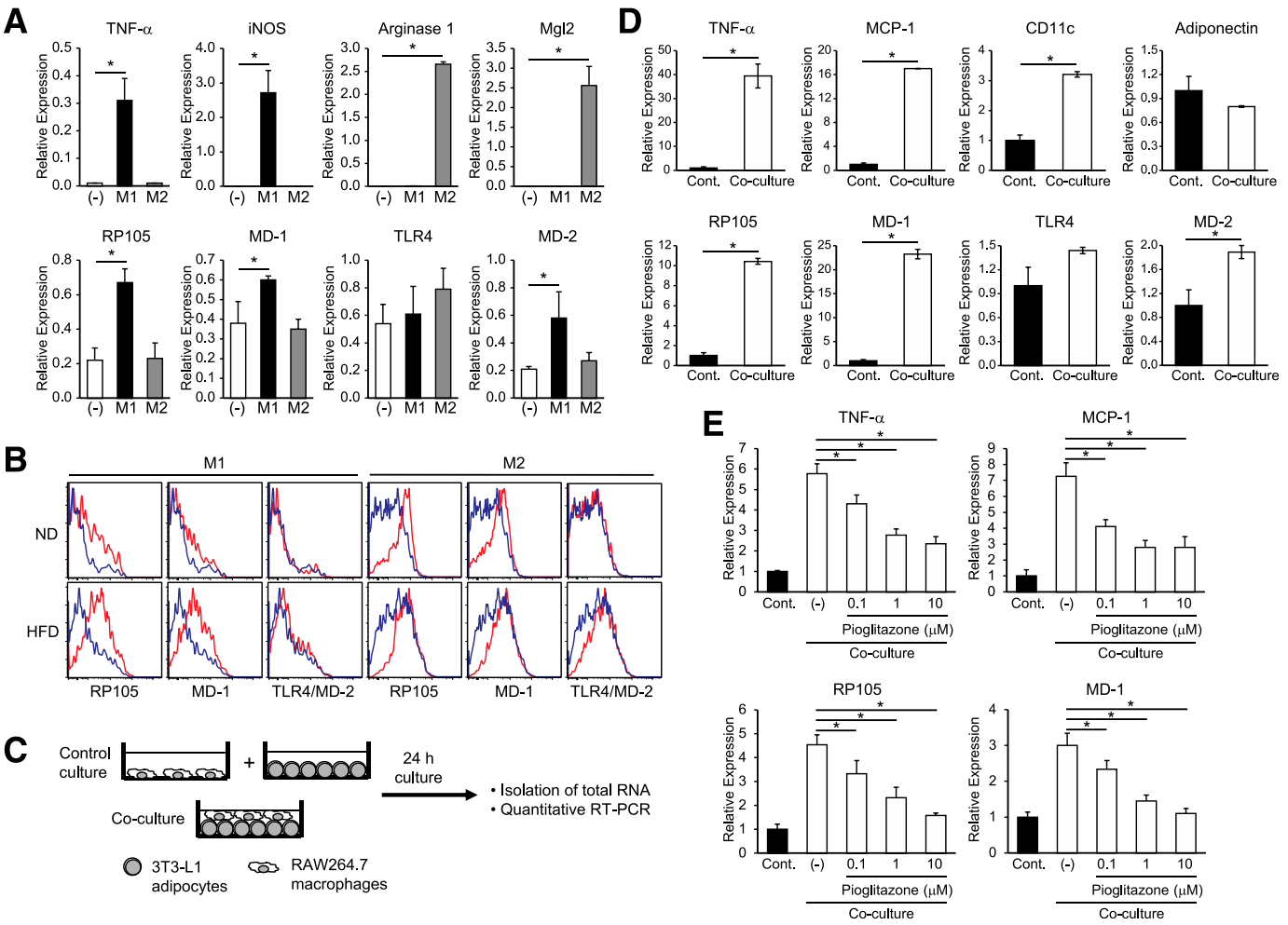

FIG. 3. Expression of RP105 and MD-1 in M1 macrophages is regulated by HFD and adipocytes. *A*: RT-qPCR of M1 markers (TNF-α and inducible nitric oxide synthase [iNOS]), M2 markers (arginase 1 and Mgl2), RP105, MD-1, TLR4, and MD-2 mRNA in differentiated M1 and M2 macrophages (n = 3 per group). (−), undifferentiated BMMs. *P < 0.05 vs. (−). *B*: Flow cytometry analysis of RP105, MD-1, and TLR4/MD-2 expression on M1 and M2 ATMs from WT mice fed with an ND or HFD for 12 weeks (blue lines, isotype control antibodies). All data are representative of at least three independent experiments. *C*: Illustration of the coculture system. *D*: RT-qPCR of TNF-α, MCP-1, CD11c, adiponectin, RP105, MD-1, TLR4, and MD-2 mRNA in the control and cocultured cells (n = 3 per group). As the control, the equal numbers of each cell were cultured separately and mixed after harvest. Data are presented relative to the expression in the control culture, set as 1. *P < 0.05 vs. control culture. *E*: RT-qPCR of TNF-α, MCP-1, RP105, and MD-1 mRNA in the control and cocultured cells with or without pioglitazone (n = 3 per group). Data are presented relative to the expression in the control culture, set as 1. (−), coculture without pioglitazone. *P < 0.05 vs. coculture without pioglitazone. Data are shown as means ± SE (*A*, *D*, and *E*). All data are representative of at least three independent experiments.

M1 but not M2 ATMs was upregulated by an HFD. The TLR4/MD-2 complex was not displayed on ATMs from both ND- and HFD-fed mice.

To understand molecular mechanisms underlying HFD-induced upregulation of RP105/MD-1 on M1 ATMs, we prepared a coculture system composed of 3T3-L1 adipocytes and macrophages (Fig. 3*C*). Using this approach, a previous study determined that saturated FAs and TNF-α in a paracrine loop could exacerbate adipose tissue inflammation (15). We observed increased expression of TNF-α, monocyte chemoattractant protein (MCP)-1, and CD11c and decreased expression of adiponectin in the cocultured cells (Fig. 3*D*). In parallel with the upregulation of TNF-α and CD11c, RP105 and MD-1 were markedly increased in the cocultured cells compared with cells in control cultures. Because 3T3-L1 cells did not express RP105 and MD-1 mRNA, macrophages were responsible for this change (data not shown). In addition, this increase was independent of TLR4 (Supplementary Fig. 6). We also observed increased expression of TLR4 and MD-2, but these changes were smaller than those of RP105 and MD-1 (Fig. 3*D*). A peroxisome proliferator–activated receptor-γ agonist pioglitazone treatment of HFD-fed WT mice decreased M1 markers and increased M2 markers in eWAT (4). Pioglitazone stimulation decreased RP105 and MD-1 mRNA, as well as TNF-α and MCP-1 mRNA induced by the coculture in a dose-dependent manner (Fig. 3*E*). Collectively, RP105 and MD-1 are associated with differentiation and responsible for activation of M1 macrophages.

RP105 KO and MD-1 KO mice have increased energy expenditure and are protected from HFD-induced obesity and hepatic steatosis. The above observations led us to analyze RP105 KO and MD-1 KO mice in the development of obesity and insulin resistance, comparing them with WT and TLR4 targeted animals. RP105 KO and MD-1 KO mice gained significantly less weight than WT and TLR4 KO mice on an HFD, whereas no significant differences were found in body weights on an ND (Fig. 4*A*). Representative photos and magnetic resonance imaging revealed decreased fat masses in RP105 KO and MD-1 KO

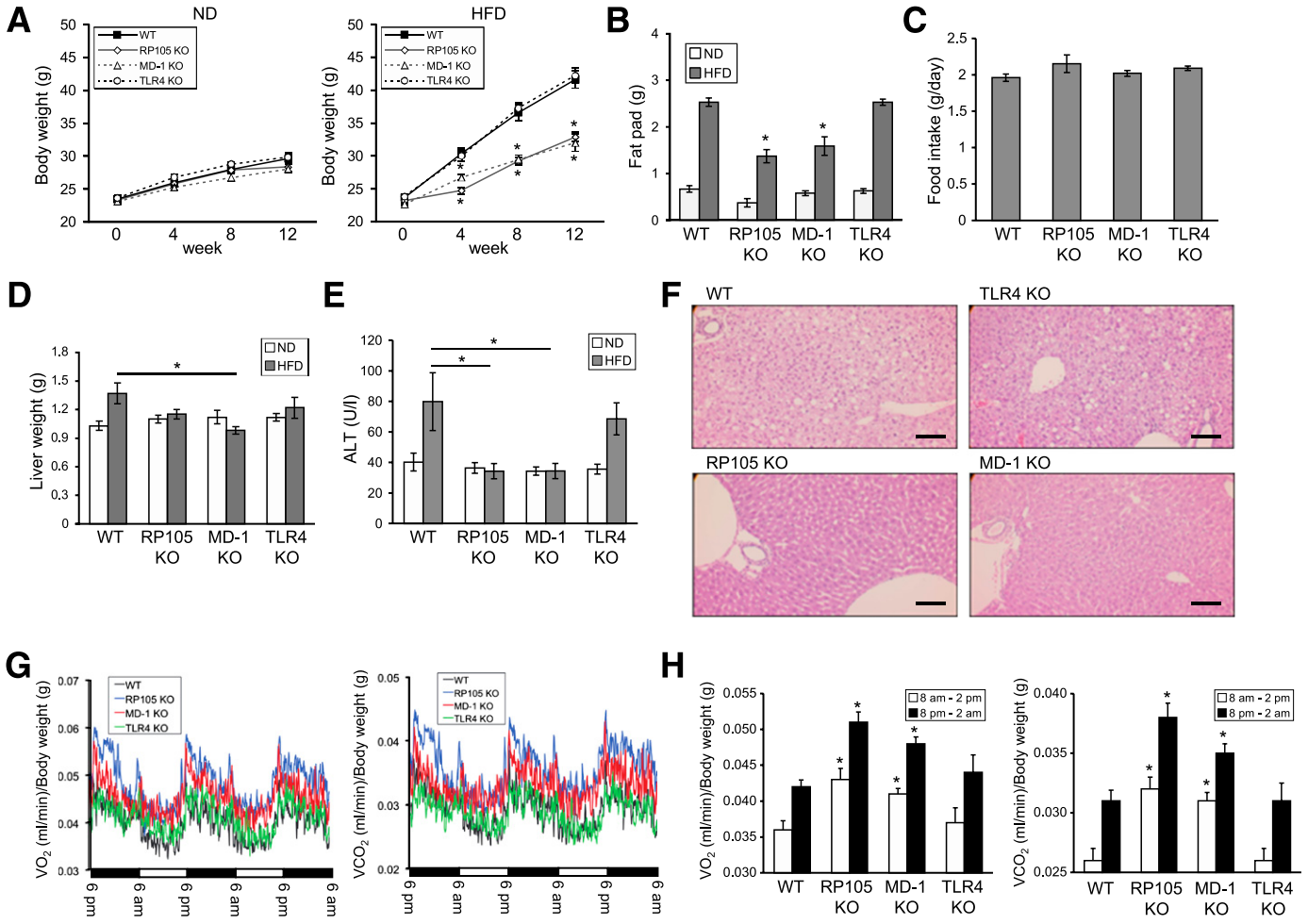

FIG. 4. RP105 KO and MD-1 KO mice with increased energy expenditure are protected from HFD-induced obesity and hepatic steatosis. ***A*****: Body weight changes of WT, RP105 KO, MD-1 KO, and TLR4 KO mice fed with an ND or HFD (*n* = 12 per group).** ***B*****: Fat-pad weights of WT, RP105 KO, MD-1 KO, and TLR4 KO mice fed with an ND or HFD for 12 weeks (*n* = 12 per group).** ***C*****: Food intake was measured for WT, RP105 KO, MD-1 KO, and TLR4 KO mice fed with an HFD for 12 weeks (*n* = 12 per group).** ***D*****: Liver weights of WT, RP105 KO, MD-1 KO, and TLR4 KO mice fed with an ND or HFD for 12 weeks (*n* = 12 per group).** ***E*****: Serum ALT levels were measured for 12-h fasting mice fed with an ND or HFD for 12 weeks (*n* = 12 per group).** ***F*****: Representative images of hematoxylin and eosin–stained sections of livers from WT, RP105 KO, MD-1 KO, and TLR4 KO mice fed with an HFD for 12 weeks. Scale bars, 200 μm.** ***G*****: Oxygen consumption (VO_2) and carbon dioxide consumption (VCO_2) were measured for WT, RP105 KO, MD-1 KO, and TLR4 KO mice fed with an HFD for 12 weeks (*n* = 6 per group). Data are shown as means.** ***H*****: The data from 8 A.M. to 2 P.M. or 8 P.M. to 2 A.M. in *G* were calculated and shown as bar graphs. Data are shown as means ± SE (*A–E* and *H*). *$P < 0.05$ vs. WT (*A*, *B*, *D*, *E*, and *H*). (A high-quality digital representation of this figure is available in the online issue.)**

mice on the HFD (Supplementary Fig. 7*A* and *B*). Fat-pad weights were similar in WT and TLR4 KO animals on the HFD but much smaller in RP105 KO and MD-1 KO mice (Fig. 4*B*). Daily food intakes were similar in all groups of mice (Fig. 4*C*).

Chronic exposure of mice to HFD causes hepatic steatosis. In WT mice, this is reflected in increased liver weights and levels of serum ALT (Fig. 4*D* and *E*). The latter response was abrogated in *Rp105* and *Md-1* gene–targeted animals. HFD induced macrovesicular steatosis in WT and TLR4 KO but not RP105 or MD-1 KO mice (Fig. 4*F*).

We further found no significant differences in locomotor activity in these mice (Supplementary Fig. 8*A*). RQ fluctuated between 0.70 and 0.75 in all groups of mice maintained on the HFD (Supplementary Fig. 8*B*). O_2 and CO_2 consumption were significantly increased through light and dark phases in RP105 KO and MD-1 KO mice, whereas these measurements were similar in WT and TLR4 KO mice (Fig. 4*G* and *H*). These data clearly demonstrated that RP105 KO and MD-1 KO mice are protected from HFD-induced obesity and hepatic steatosis, and energy expenditure is increased when RP105 and MD-1 are nonfunctional.

RP105 KO and MD-1 KO mice are protected from HFD-induced hypercholesterolemia and insulin resistance. All gene-targeted animals had reduced fasting serum cholesterol levels on the HFD (Fig. 5*A*). Chronic exposure to HFD increased fasting glucose and insulin levels in WT and TLR4 KO but not RP105 and MD-1 KO mice (Fig. 5*B* and *C*). The HFD caused insulin resistance and impaired glucose tolerance in WT mice, whereas the KO mice seemed to be more insulin sensitive and to have better glucose tolerance (Fig. 5*D* and *E*). Insulin sensitivities of MD-1 KO and TLR4 KO but not RP105 KO mice significantly improved compared with WT mice (Fig. 5*F*, *left*). Significant differences between WT and the KO mice were not observed in the GTT (Fig. 5*F*, *right*).

HFD-induced macrophage infiltration and adipose tissue inflammation are attenuated in RP105 KO and MD-1 KO mice. The improved insulin action in RP105- or MD-1–deficient mice led us to investigate cell subsets in

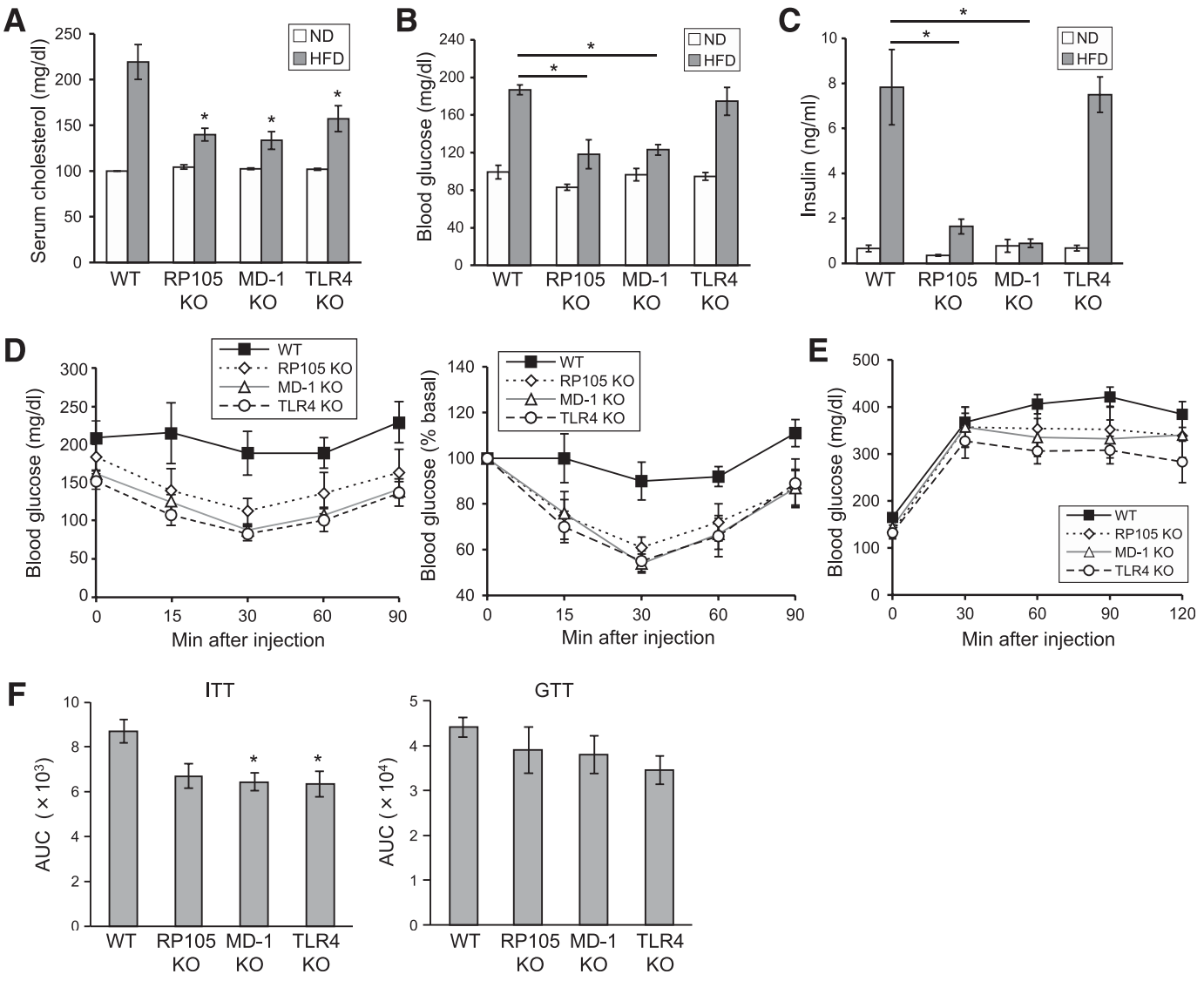

FIG. 5. RP105 KO and MD-1 KO mice are protected from HFD-induced hypercholesterolemia and insulin resistance. *A*: Serum cholesterol levels were measured for 12-h fasting mice fed with an ND or HFD for 12 weeks (n = 12 per group). *B* and *C*: Serum glucose (*B*) and insulin (*C*) levels were measured after a 12-h fasting in mice fed with an ND or HFD for 12 weeks (n = 12 per group). *D*: An ITT was performed after 3 h of fasting in mice fed with an HFD for 12 weeks (n = 6 per group). *Left*: Data are presented as absolute values. *Right*: Data are presented relative to the values of 0 min (preinjection), set as 100%. *E*: A GTT was performed after 12 h of fasting in mice fed with an HFD for 12 weeks (n = 6 per group). Data are shown as means ± SE. *F*: Area under the curve (AUC) graphs of ITT (*left*) and GTT (*right*) tests are presented. Data are shown as means ± SE. *P < 0.05 vs. WT.

adipose tissue and assess their expression of inflammatory genes. Compared with WT mice on an HFD, RP105 KO and MD-1 KO mice had severe reductions in the number of SVF cells and F4/80$^+$ cells in eWAT (Fig. 6*A* and *B*). In contrast, adipose tissue from TLR4 KO mice on an HFD exhibited mild reductions in these numbers compared with WT mice. The number of M1 ATMs (F4/80$^+$/CD11c$^+$/CD206$^-$) was markedly reduced in RP105- or MD-1–deficient eWAT compared with WT mice (Fig. 6*C*). M2 ATMs (F4/80$^+$/CD11c$^-$/CD206$^+$) also accumulated in eWAT during obesity (Fig. 6*C*). Their numbers were significantly reduced in RP105 KO, MD-1 KO, and TLR4 KO mice compared with WT mice. An HFD induced a large increase in ATMs, which form a crown-like structure around adipocytes in WT mice (Fig. 6*D*). We observed severe reductions of ATMs in the eWAT of RP105 KO and MD-1 KO mice. TLR4-deficient eWAT showed mild reductions in ATMs compared with WT mice. Expression of inflammatory genes, such as TNF-α, MCP-1, and IKKε, was increased by an HFD compared with an ND in WT and TLR4 KO mice (Fig. 6*E*). TNF-α and MCP-1 mRNAs also were increased by an HFD in subcutaneous and retroperitoneal adipose tissues of WT mice (Supplementary Fig. 1). In contrast, such increases were not observed in the eWAT of RP105 KO and MD-1 KO mice (Fig. 6*E*). Consistent with the reduction in the number of F4/80$^+$ cells and M1 macrophages, expression of F4/80 and CD11c mRNA was decreased in RP105- or MD-1–deficient eWAT fed with an HFD. Adiponectin expression was decreased by an HFD in WT and TLR4 KO mice but not RP105 or MD-1 deficiency. In addition, the lack of RP105/MD-1 did not affect the differentiation of BMMs into M1 subset induced by LPS plus interferon-γ (Fig. 6*F*).

We examined the activity of some of the key signaling molecules involved in adipose tissue inflammation and insulin resistance. To assess the role of Jun NH2-terminal kinase (JNK) (26,27), lysates from eWAT or SVF were

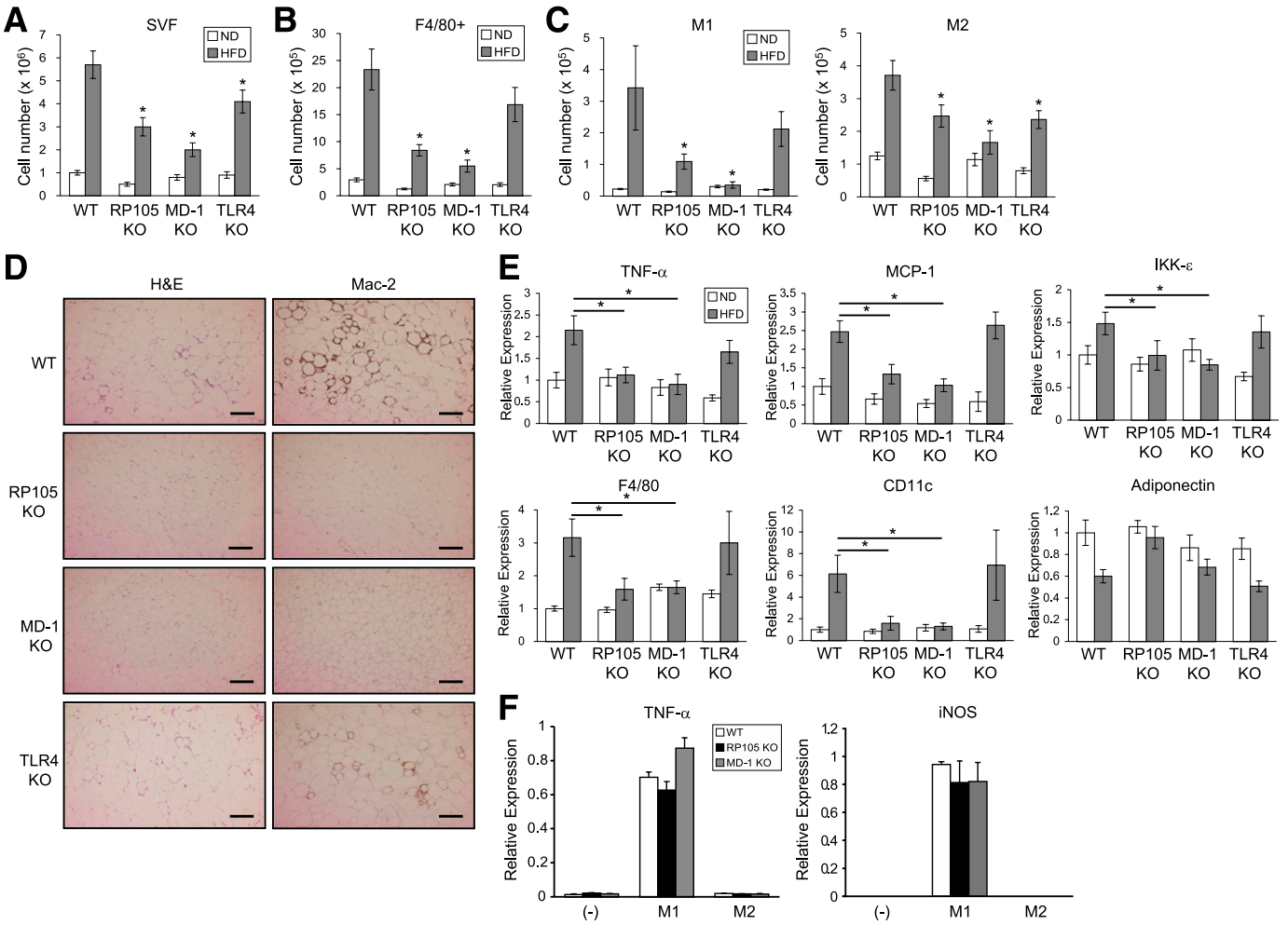

FIG. 6. Obesity-induced macrophage infiltration and adipose tissue inflammation are attenuated in RP105 KO and MD-1 KO mice. *A* and *B*: Cell number of SVF cells (*A*) and F4/80$^+$ cells (*B*) in eWAT from WT, RP105 KO, MD-1 KO, and TLR4 KO mice fed with an ND or HFD for 12 weeks (n = 12 per group). *C*: Cell number of M1 (*left*) and M2 (*right*) macrophages in eWAT from WT, RP105 KO, MD-1 KO, and TLR4 KO mice fed with an ND or HFD for 12 weeks (n = 12 per group). *D*: Representative histological images of eWAT from WT, RP105 KO, MD-1 KO, and TLR4 KO mice fed with an HFD for 12 weeks stained with hematoxylin and eosin (H&E) and Mac-2. Scale bars, 100 μm. *E*: RT-qPCR of TNF-α, MCP-1, IKKε, F4/80, CD11c, and adiponectin mRNA in eWAT from WT, RP105 KO, MD-1 KO, and TLR4 KO mice fed with an ND or HFD for 12 weeks (n = 12 per group). *F*: BMMs from WT, RP105 KO, and MD-1 KO mice were differentiated into M1 or M2 macrophages. After 24 h, expression of M1 markers in the stimulated cells was measured by RT-qPCR. Data are shown as means ± SE (*A–C*, *E*, and *F*). *P < 0.05 vs. WT. (A high-quality digital representation of this figure is available in the online issue.)

immunoblotted with a phospho-JNK antibody. We did not observe significant increased phospho-JNK in the eWAT from WT and the KO mice by HFD (Supplementary Fig. 9*A*, *left*). An HFD produced increased phospho-JNK in SVF from WT mice (Supplementary Fig. 9*A*, *right*). Of interest, TLR4 KO but not RP105 KO and MD-1 KO mice exhibited reduced levels of phospho-JNK in SVF by HFD, suggesting that TLR4/MD-2 but not RP105/MD-1 is important for HFD-induced JNK activation. An HFD induced IκBα degradation in SVF from WT but not RP105 KO, MD-1 KO, and TLR4 KO mice, suggesting that nuclear factor (NF)-κB is activated by both TLR4/MD-2 and RP105/MD-1 (Supplementary Fig. 9*B*). IKKε is a direct transcriptional target of NF-κB (28). IKKε phosphorylation was investigated by Western blotting, as a surrogate to assay activation of the kinase. IKKε expression in eWAT was similarly increased after an HFD in WT, RP105 KO, MD-1 KO, and TLR4 KO mice (Supplementary Fig. 9*C*). Of interest, HFD increased levels of phospho-IKKε in eWAT from WT, RP105 KO, and MD-1 KO, but not TLR4 KO, mice, suggesting that IKKε phosphorylation after an HFD is downstream TLR4 but not RP105 signaling.

Because TLRs can regulate inflammatory activation, we wondered whether RP105 KO mice might also be hyporesponsive to acute inflammatory stimuli. LPS injection led to a profound elevation in proinflammatory genes in the SVF (Fig. 7). However, the levels of these genes were not affected by RP105 deficiency. Collectively, the RP105/MD-1 complex contributes to the development of diet-induced chronic, low-grade adipose tissue inflammation.

The RP105/MD-1 complex is not involved in palmitic and stearic acid–induced macrophage activation. Palmitic acid is one of the most abundant saturated FAs in plasma and is substantially elevated by an HFD (29). Furthermore, palmitic acid has been reported to be an endogenous TLR4 ligand (15–17). BSA–palmitic acid, but not BSA alone, increased TNF-α mRNA in WT BMMs (Fig. 8*A*, *upper panel*). TLR4-deficient BMMs showed a lower increase of TNF-α mRNA than WT upon BSA–palmitic acid stimulation. In contrast, WT, RP105-deficient, and MD-1–deficient BMMs

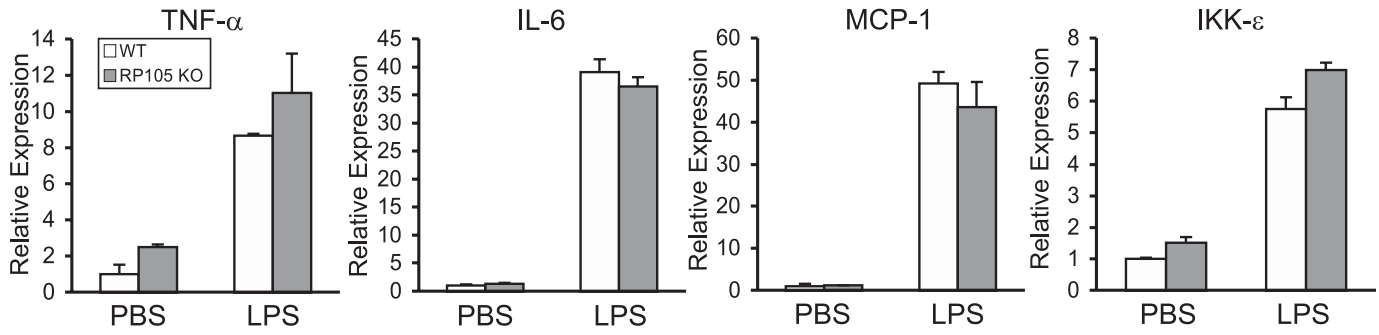

FIG. 7. RP105 does not mediate LPS-induced inflammatory responses in SVF of eWAT. WT and RP105 KO mice (n = 3 per group) were injected with LPS (50 μg/mice) intraperitoneally. After 3 h, SVF was isolated from eWAT and expression of TNF-α, IL-6, MCP-1, and IKKε mRNA was measured by RT-qPCR. Data are presented relative to the expression in PBS-injected WT mice, set as 1. Data are shown as means ± SE. Data are representative of at least two independent experiments.

generated similar levels of TNF-α mRNA in response to BSA–palmitic acid. BMMs also were stimulated with other saturated FAs. Upon 100 μmol/L of BSA–stearic acid stimulation, WT, RP105-deficient, and MD-1–deficient BMMs similarly increased levels of TNF-α mRNA, and this was dependent on TLR4 (Fig. 8*A*, *middle panel*). However, upon 200 μmol/L of BSA–stearic acid stimulation, we did not observe the TLR4 dependency. Although lauric acid induces NF-κB activation in RAW264.7 cells via TLR4 (30), we did not observe significantly increased TNF-α mRNA by BSA–lauric acid in BMMs from WT and all the KO mice (Fig. 8*A*, *lower panel*). Thus, although palmitic and stearic acids activate innate immunity via TLR4/MD-2, a different ligand must be recognized by RP105/MD-1 and be responsible for most of obesity-related inflammation (Fig. 8*B*).

DISCUSSION

Here, we provided evidence that RP105/MD-1 plays a major role in regulating adipose tissue inflammation and metabolic disorders. Many detrimental consequences of an HFD were ameliorated by targeting genes encoding for RP105 or MD-1. TLR4 KO mice showed reduced HFD-induced adipose tissue inflammation (Fig. 6), but our results clearly revealed more requirements of RP105/MD-1 than TLR4/MD-2 in the induction of adipose tissue inflammation and obesity. The higher levels of cell surface and transcript expression of RP105/MD-1 in eWAT might simply reflect the requirements of RP105/MD-1 (Figs. 1–3). As is demonstrated, however, RP105/MD-1 plays unique, TLR4-independent roles in adipose tissue inflammation, and a ligand and signaling pathway of RP105/MD-1 must be different from those of TLR4/MD-2 (Fig. 8*A* and Supplementary Fig. 9). A dietary or endogenous ligand other than palmitic and stearic acids might trigger upregulation of RP105 on macrophages that, in turn, accumulate in adipose tissue. The underlying mechanisms require more investigation, but some aspects are clear.

Both MD-1 and MD-2 are members of the same lipid-recognition family (31), and MD-2 is essential for LPS recognition (7). Crystal structure analyses revealed that MD-1 could recognize lipid-like molecules (32,33). An endogenous ligand for RP105/MD-1 must be something other than palmitic and stearic acids (Fig. 8*A*), inducing adipose tissue inflammation by RP105/MD-1 signaling pathway. Otherwise, it might not necessarily be a saturated FA, since some proteins and other components induce sterile inflammation via TLR4/MD-2. Other lipids or components derived from inflamed tissues might stimulate RP105/MD-1 in adipose tissue inflammation. Identification of ligands that promote adipose tissue inflammation via RP105/MD-1 would be an important achievement.

Although other TLRs have a Toll/interleukin-1 receptor (TIR) domain in the intracellular segment, RP105 has only 11 amino acids in that portion (24). This suggests that RP105 requires another molecule to transmit its signal. In B cells, CD19 regulates RP105 but not TLR4 signaling (34). The MyD88 and TRIF adaptors are involved in TLR4 (5) but not RP105 signaling (data not shown). However, little is known about how RP105 regulates chronic inflammation. The NF-κB pathway plays a crucial role in obesity-associated inflammation. HFD activates NF-κB in fat and liver and increases IKKε expression in M1 macrophages (28). IKKε KO mice do not gain weight on an HFD with increased energy expenditure (28). In addition, IKKε KO mice are protected from diet-induced hepatic steatosis, macrophage infiltration into adipose tissue, and increased expression of inflammatory genes in eWAT. The similarities between these changes and ones we attributed to RP105/MD-1 are intriguing. However, although both TLR4 and RP105 are required for HFD-induced NF-κB activation (Supplementary Fig. 9*B*), IKKε may be activated in the downstream of TLR4 but not the RP105 pathway by HFD (Supplementary Fig. 9*C*). In addition, TLR4 but not RP105 may activate JNK pathway in obese mice (Supplementary Fig. 9*A*). Thus, RP105 shares some signaling pathways with TLR4 but must have distinct ones from TLR4.

Levels of RP105 mRNA in SVF and macrophages were dramatically increased by HFD and coculture with adipocytes, respectively. We did not record similar changes in spleen, bone marrow, or even other immune cells in eWAT (data not shown). This raises the possibility of a self-amplifying, feed-forward mechanism of diet-induced inflammation. Processing or production of an RP105/MD-1 ligand by adipocytes might recruit and activate macrophages that produce cytokines capable of promoting obesity and systemic metabolic changes.

The dramatic changes in metabolic status and inflammation in RP105 KO and MD-1 KO mice we observed might have resulted from lower body weights in these KO mice. However, deletion of some genes prevents inflammation and insulin resistance but not weight gain from an HFD (35–37). Others (16) and we have demonstrated that TLR4 KO mice on an HFD have restored insulin resistance but continue to gain weight. Blunting that response to diet is desirable and unique to RP105/MD-1.

The RP105/MD-1 complex is not expressed in $CD45^-$ nonleukocytes in eWAT and RP105 expression is largely

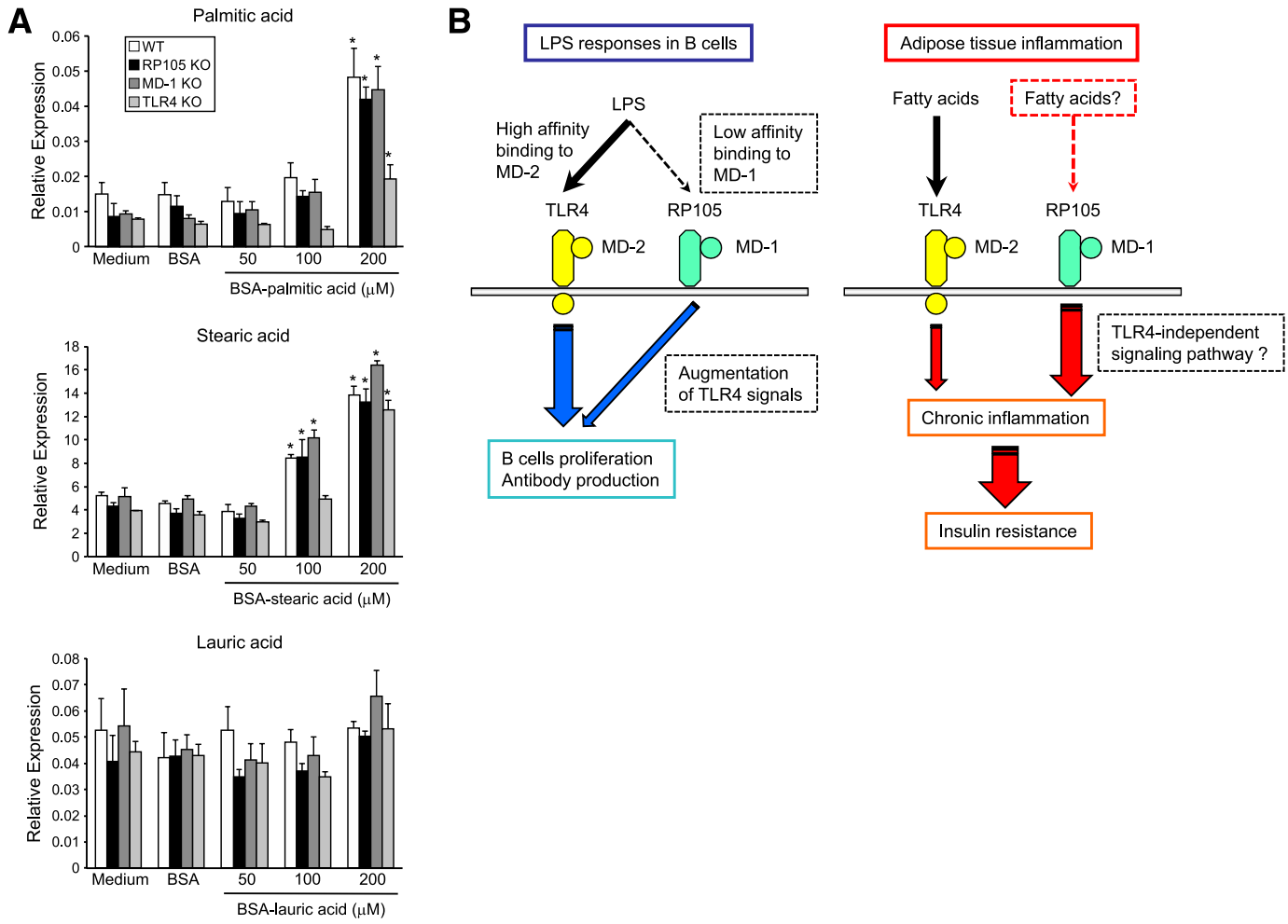

FIG. 8. Palmitate activates TLR4 but not RP105/MD-1 signaling. *A*: FAs (palmitic, stearic, and lauric acids) need to be conjugated to FA-free BSA to increase solubility. BMMs from WT, RP105 KO, MD-1 KO, and TLR4 KO mice were stimulated with the FAs conjugate to BSA or BSA control (BSA) for 24 h. Expression of TNF-α mRNA in the stimulated BMMs was measured by RT-qPCR (n = 3 per group). Data are shown as means ± SE. *P < 0.05 vs. BSA control. Similar results were obtained in three independent experiments. *B*: Hypothetical model of RP105/MD-1 activation in LPS responses in B cells and adipose tissue inflammation. The TLR4/MD-2 complex is essential for LPS recognition and responses. The RP105/MD-1 also could recognize LPS by low affinity and augment TLR4-dependent LPS responses in B cells. On the other hand, RP105/MD-1 might contribute to the development of adipose tissue inflammation and insulin resistance by palmitate-TLR4–independent manner.

restricted to the immune system (24). However, involvement of other cell types is possible. Signaling mediated by MyD88 can mediate HFD-induced leptin and insulin resistance in the central nervous system (38). Another report (39) suggests that TLR4 signaling in hematopoietic cells is important for obesity-associated insulin resistance. Although RP105 transcripts were low in the brain (data not shown), we observed that an HFD increased RP105 mRNA in the liver, brown adipose tissue, and skeletal muscle. Additional investigation will reveal if RP105/MD-1 has roles in those tissues.

To conclude, the RP105/MD-1 complex mediates much of the weight gain, insulin resistance, and sterile inflammation that result from exposure to an HFD. Future studies will clarify a precise ligand and signaling pathway of RP105/MD-1, which link this complex and adipose tissue inflammation.

ACKNOWLEDGMENTS

This study was supported by grants from Grant-in-Aid for Scientific Research from the Ministry of Education, Culture, Sports, Science, and Technology of the Japanese Government (20390141 and 22117509); Hokuriku Innovation Cluster for Health Science (to K.Ta.); the Uehara Memorial Foundation (to Y.N.); the Novartis Foundation (Japan) for the Promotion of Science (to Y.N.); and Takeda Science Foundation (to Y.N.).

No potential conflicts of interest relevant to this article were reported.

Y.W. conducted the experiments and wrote the manuscript. T.N. conducted the experiments. S.I. contributed to the knockout mice analysis. S.F., I.U., and K.To. contributed to the metabolic measurement data. K.Ts. contributed to the immunohistochemistry data. Y.I., T.W., and T.Sa. contributed to the energy expenditure data. Y.H., H.I., H.K., M.Sh., and M.Sa. contributed to the human study. T.Su. and Y.O. contributed to the coculture data. K.Ta. was involved in project planning, financing, and supervision. Y.N. conceived the study, conducted the experiments, and wrote the manuscript. S.A. and K.M. provided the knockout mice. Y.N. is the guarantor of this work and, as such, had full access to all of the data in the study and takes responsibility for the integrity of the data and the accuracy of the data analysis.

The authors sincerely thank Toyama Prefecture for supporting their laboratory. The authors also thank Drs. Paul W. Kincade, Oklahoma Medical Research Foundation, and Masao Kimoto, Saga University, for critical review of the manuscript. The authors thank Drs. Yoshikatsu Hirai, Ai Kariyone, Masashi Ikutani, and Tsutomu Yanagibashi, University of Toyama, for helpful suggestions. Ena Taniguchi, Yumi Miyahara, and Satoko Katsunuma, University of Toyama, are thanked for their technical assistance. The authors appreciate the secretarial assistance provided by Maki Sasaki and Ryoko Sugimoto, University of Toyama.

REFERENCES

1. Hotamisligil GS, Erbay E. Nutrient sensing and inflammation in metabolic diseases. Nat Rev Immunol 2008;8:923–934
2. Olefsky JM, Glass CK. Macrophages, inflammation, and insulin resistance. Annu Rev Physiol 2010;72:219–246
3. Lumeng CN, Bodzin JL, Saltiel AR. Obesity induces a phenotypic switch in adipose tissue macrophage polarization. J Clin Invest 2007;117:175–184
4. Fujisaka S, Usui I, Bukhari A, et al. Regulatory mechanisms for adipose tissue M1 and M2 macrophages in diet-induced obese mice. Diabetes 2009; 58:2574–2582
5. Kawai T, Akira S. The role of pattern-recognition receptors in innate immunity: update on Toll-like receptors. Nat Immunol 2010;11:373–384
6. Hoshino K, Takeuchi O, Kawai T, et al. Cutting edge: Toll-like receptor 4 (TLR4)-deficient mice are hyporesponsive to lipopolysaccharide: evidence for TLR4 as the Lps gene product. J Immunol 1999;162:3749–3752
7. Nagai Y, Akashi S, Nagafuku M, et al. Essential role of MD-2 in LPS responsiveness and TLR4 distribution. Nat Immunol 2002;3:667–672
8. Miyake K, Yamashita Y, Hitoshi Y, Takatsu K, Kimoto M. Murine B cell proliferation and protection from apoptosis with an antibody against a 105-kD molecule: unresponsiveness of X-linked immunodeficient B cells. J Exp Med 1994;180:1217–1224
9. Miyake K, Shimazu R, Kondo J, et al. Mouse MD-1, a molecule that is physically associated with RP105 and positively regulates its expression. J Immunol 1998;161:1348–1353
10. Ogata H, Su I, Miyake K, et al. The toll-like receptor protein RP105 regulates lipopolysaccharide signaling in B cells. J Exp Med 2000;192:23–29
11. Nagai Y, Shimazu R, Ogata H, et al. Requirement for MD-1 in cell surface expression of RP105/CD180 and B-cell responsiveness to lipopolysaccharide. Blood 2002;99:1699–1705
12. Nagai Y, Kobayashi T, Motoi Y, et al. The radioprotective 105/MD-1 complex links TLR2 and TLR4/MD-2 in antibody response to microbial membranes. J Immunol 2005;174:7043–7049
13. Kono H, Rock KL. How dying cells alert the immune system to danger. Nat Rev Immunol 2008;8:279–289
14. Chen GY, Nuñez G. Sterile inflammation: sensing and reacting to damage. Nat Rev Immunol 2010;10:826–837
15. Suganami T, Nishida J, Ogawa Y. A paracrine loop between adipocytes and macrophages aggravates inflammatory changes: role of free fatty acids and tumor necrosis factor alpha. Arterioscler Thromb Vasc Biol 2005;25:2062–2068
16. Shi H, Kokoeva MV, Inouye K, Tzameli I, Yin H, Flier JS. TLR4 links innate immunity and fatty acid-induced insulin resistance. J Clin Invest 2006;116: 3015–3025
17. Suganami T, Tanimoto-Koyama K, Nishida J, et al. Role of the Toll-like receptor 4/NF-kappaB pathway in saturated fatty acid-induced inflammatory changes in the interaction between adipocytes and macrophages. Arterioscler Thromb Vasc Biol 2007;27:84–91
18. Vandanmagsar B, Youm YH, Ravussin A, et al. The NLRP3 inflammasome instigates obesity-induced inflammation and insulin resistance. Nat Med 2011;17:179–188
19. Wen H, Gris D, Lei Y, et al. Fatty acid-induced NLRP3-ASC inflammasome activation interferes with insulin signaling. Nat Immunol 2011;12:408–415
20. Nakamura T, Furuhashi M, Li P, et al. Double-stranded RNA-dependent protein kinase links pathogen sensing with stress and metabolic homeostasis. Cell 2010;140:338–348
21. Oh DY, Talukdar S, Bae EJ, et al. GPR120 is an omega-3 fatty acid receptor mediating potent anti-inflammatory and insulin-sensitizing effects. Cell 2010;142:687–698
22. Rubin CS, Hirsch A, Fung C, Rosen OM. Development of hormone receptors and hormonal responsiveness in vitro: insulin receptors and insulin sensitivity in the preadipocyte and adipocyte forms of 3T3-L1 cells. J Biol Chem 1978;253:7570–7578
23. Ichioka M, Suganami T, Tsuda N, et al. Increased expression of macrophage-inducible C-type lectin in adipose tissue of obese mice and humans. Diabetes 2011;60:819–826
24. Miyake K, Yamashita Y, Ogata M, Sudo T, Kimoto M. RP105, a novel B cell surface molecule implicated in B cell activation, is a member of the leucine-rich repeat protein family. J Immunol 1995;154:3333–3340
25. Nishimura S, Manabe I, Nagasaki M, et al. CD8+ effector T cells contribute to macrophage recruitment and adipose tissue inflammation in obesity. Nat Med 2009;15:914–920
26. Hirosumi J, Tuncman G, Chang L, et al. A central role for JNK in obesity and insulin resistance. Nature 2002;420:333–336
27. Solinas G, Vilcu C, Neels JG, et al. JNK1 in hematopoietically derived cells contributes to diet-induced inflammation and insulin resistance without affecting obesity. Cell Metab 2007;6:386–397
28. Chiang SH, Bazuine M, Lumeng CN, et al. The protein kinase IKKepsilon regulates energy balance in obese mice. Cell 2009;138:961–975
29. Boden G. Interaction between free fatty acids and glucose metabolism. Curr Opin Clin Nutr Metab Care 2002;5:545–549
30. Lee JY, Sohn KH, Rhee SH, Hwang D. Saturated fatty acids, but not unsaturated fatty acids, induce the expression of cyclooxygenase-2 mediated through Toll-like receptor 4. J Biol Chem 2001;276:16683–16689
31. Inohara N, Nuñez G. ML: a conserved domain involved in innate immunity and lipid metabolism. Trends Biochem Sci 2002;27:219–221
32. Harada H, Ohto U, Satow Y. Crystal structure of mouse MD-1 with endogenous phospholipid bound in its cavity. J Mol Biol 2010;400:838–846
33. Yoon SI, Hong M, Han GW, Wilson IA. Crystal structure of soluble MD-1 and its interaction with lipid IVa. Proc Natl Acad Sci USA 2010;107:10990–10995
34. Yazawa N, Fujimoto M, Sato S, et al. CD19 regulates innate immunity by the toll-like receptor RP105 signaling in B lymphocytes. Blood 2003;102:1374–1380
35. Kanda H, Tateya S, Tamori Y, et al. MCP-1 contributes to macrophage infiltration into adipose tissue, insulin resistance, and hepatic steatosis in obesity. J Clin Invest 2006;116:1494–1505
36. Lesniewski LA, Hosch SE, Neels JG, et al. Bone marrow-specific Cap gene deletion protects against high-fat diet-induced insulin resistance. Nat Med 2007;13:455–462
37. Weisberg SP, Hunter D, Huber R, et al. CCR2 modulates inflammatory and metabolic effects of high-fat feeding. J Clin Invest 2006;116:115–124
38. Kleinridders A, Schenten D, Könner AC, et al. MyD88 signaling in the CNS is required for development of fatty acid-induced leptin resistance and diet-induced obesity. Cell Metab 2009;10:249–259
39. Saberi M, Woods NB, de Luca C, et al. Hematopoietic cell-specific deletion of toll-like receptor 4 ameliorates hepatic and adipose tissue insulin resistance in high-fat-fed mice. Cell Metab 2009;10:419–429